Food and Chemical Toxicology 203 (2025) 115594

Contents lists available at ScienceDirect

Food and Chemical Toxicology

journal homepage: www.elsevier.com/locate/foodchemtox

Therapeutic effects of apilarnil, a bee product, on apoptosis and autophagy in cisplatin-induced rat ovarian toxicity

Kübra Tuğçe Kalkan [a,*], Halime Tozak Yıldız [a], Betül Yalçın [b], Özge Cengiz Mat [c], Gözde Özge Önder [c], Arzu Yay [c]

[a] Department of Histology and Embryology, Faculty of Medicine, Kırşehir Ahi Evran University, Merkez, 40100, Kırşehir, Turkey
[b] Department of Histology and Embryology, Faculty of Medicine, Adıyaman University, Merkez, 02040, Adıyaman, Turkey
[c] Department of Histology and Embryology, Faculty of Medicine, Erciyes University, Talas, 38030, Kayseri, Turkey

ARTICLE INFO

Handling editor: Dr. Bryan Delaney

Keywords:
Cisplatin
Apilarnil
Apitherapy
Ovary
Rat

ABSTRACT

Objective: Cisplatin (CP) is a platinum derivative used to treat ovarian, breast, testicular, and bladder cancers. As one of the apitherapy products, apilarnil (API) contains androgenic hormones and is extremely chemically complex. CP alterations in rats' ovarian tissue were evaluated by API, a possible therapeutic medicine.
Methods: Each group of female rats consisted of seven rats. One dosage of 7.5 mg/kg/day CP was administered intraperitoneally to the CP group. The API group received 0.5 g/kg/day of apilarnil orally for ten days. Ovarian tissues were then examined histopathologically, immunohistochemically, and biochemically. Beclin-1, p62, and LC-3, along with Caspase-3 and AIF, were immunohistochemically determined. ELISA tests were performed on MDA, GSH-PX, SOD, CAT, AMH, FSH, and LH levels.
Results: The CP group had significantly fewer primordial follicles than the control group. This group also showed edema, vacuolization, and congested blood vessels. The findings were improved by the API therapy. Furthermore, API was shown to restore Beclin-1 and p62 levels, as well as Caspase-3 and AIF expression, which had all increased in the CP group. API reduced MDA, which had grown due to toxicity, whereas SOD and CAT levels improved. Furthermore, it greatly increased AMH levels, which are an indicator of ovarian reserve and decrease.
Conclusions: This study concluded that API, an organic chemical used in apitherapy, can restore damage to the female reproductive system caused by CP treatment. Apilarnil is a promising therapy for female gonadal failure.

1. Introduction

Cisplatin (CP) is an effective chemotherapy drug containing a heavy metal called platinum (Lee et al., 2020). The drug is often used to treat a range of solid tumors, including malignancies of the colon, head, lung, breast, testicles, ovary, and uterus (Jang et al., 2016). CP toxicity is not limited to tumor cells but also affects the biological functions of healthy cells (Khan et al., 2012). The underlying cause of CP-induced toxicity remains undetermined, however, it is believed to involve multiple factors such as increased DNA damage, oxidative stress, inflammation, and apoptosis (Lee et al., 2020). CP induces major damage to tissues and side effects. The most prevalent type of toxicity is nephrotoxicity, which leads to acute kidney injury by triggering oxidative stress, inflammation, and death in kidney cells. Furthermore, ear toxicities such as ototoxicity and hearing loss are commonly recorded. Mucositis is unique among gastrointestinal side effects. Haematological toxicity can cause anaemia, leukopenia, or thrombocytopenia. İn addition CP may negatively affect other organs, including hepatotoxicity, cardiotoxicity, and neurotoxicity (Perše, 2021; Romani, 2022). Reactive oxygen metabolites released during CP metabolism are believed to degrade tissue in the reproductive system (Lee et al., 2020; Spears et al., 2019). CP adversely affects ovarian reserve and fertility, including reduced primordial follicle number and Anti-Müllerian hormone (AMH) levels (Atli et al., 2017). Autophagy is a critical physiological system that controls several transcription factors and signalling pathways to promote various physiological processes, such as starvation, differentiation, and stress-induced cell survival (Hama et al., 2023). A component of the autophagic process in damaged tissue appears in the expression levels of the proteins Beclin1, P62, and LC-3 (Bortnik and Gorski, 2017). Apoptotic and autophagic cell death have bilateral interactions. As an illustration, certain pro-apoptotic signals trigger autophagy. Conversely, autophagy is suppressed by several antiapoptotic signals. The autophagy pathway can regulate interactions between genes that control apoptosis

This article is part of a special issue entitled: New Approaches published in Food and Chemical Toxicology.

* Corresponding author.

https://doi.org/10.1016/j.fct.2025.115594
Received 9 July 2024; Received in revised form 1 June 2025; Accepted 5 June 2025
Available online 18 June 2025

Abbreviation list

CP	Cisplatin
API	Apilarnil
AMH	Anti-Müllerian hormone
FSH	Follicle-stimulating hormone
LH	Luteinizing hormone
H&E	Hematoxylin and eosin
AIF	Apoptosis-inducing factor
PBS	Phosphate-buffered saline
MDA	Malondialdehyde
SOD	Superoxide dismutase
CAT	Catalase
GSH-PX	Glutathione peroxidase
ROS	Reactive oxygen species

(Kumariya et al., 2021).

Apilarnil (API) is a product of the pupal stage of the drone larva. This cream-coloured, viscous bee product can be obtained for a duration of three to seven days collected and refined to attain homogeneity (Rutka et al., 2021). API consists of 65–75 % water, 9–12 % protein, 6–12 % carbohydrates, 3.5–8 % fatty acids and lipids, minerals (K, Na, Ca, Mg), as well as essential amino acids (threonine, leucine, isoleucine, and methionine) (Erdem and Özkök, 2018; Sawczuk et al., 2019). API, which has antiviral and antibacterial actions, is also a powerful antioxidant due to its high polyphenol content (Kumariya et al., 2021). Because of its strong catabolic effect on the body, this bee product is a potent stimulant of oxidative processes that generate energy (Babacan and Ayar, 2024). The neuroprotective properties of API against brain damage and other neurological conditions are well known(Hamamci et al., 2020). In addition to skin diseases, it is also used for the relief of illnesses of the digestive and respiratory systems (Erdem and Özkök, 2018). High levels of androgenic hormones produced by API also affect the reproductive systems of males and females. It is beneficial for male infertility, sperm abnormalities, and boosting sperm count, as well as premenstrual syndrome, amenorrhea, primary dysmenorrhea, and neuroendocrine challenges related to menopause (Erdem and Özkök, 2018). The effectiveness of API in the female reproductive system has not been extensively studied in the literature. Following that, the current study will investigate at the effects of API treatment on ovarian tissue using histopathological, immunohistochemical, and biochemical approaches, which have the potential to be therapeutic for CP toxicity.

2. Materials and methods

2.1. Animal details

Twenty-eight adult female Wistar-Albino rats, ranging between 150 and 250 g, were kept in stress-free accommodation with full access to water and standard food. The Erciyes University Animal Experiments Local Ethics Committee has agreed to our experimental protocols (Ethics Committee No, 2022-22/188). The research was conducted in line with the Declaration of Helsinki and the National Institutes of Health's Guide for the Care and Use of Laboratory Animals (Ashcroft, 2008).

2.2. Experimental design

Four distinct categories of rats were set up: Apilarnil (API; n = 7), Cisplatin (CP; n = 7), Cisplatin + Apilarnil (CP + API; n = 7), and Control (n = 7). The rats in the control group did not receive any care. Intraperitoneal injection (i.p.) of 7.5 mg/kg/day CP (Sigma-Aldrich, Saint Louis, MO) dispersed into normal saline provided to the CP group as a single dose (Aboraya et al., 2022). For 10 days, the API group was conducted 0.5 g/kg/day of Apilarnil (Dalakçım beekeeping, business code: TR 400000159086) orally (Hamamci et al., 2020). For 10 days, the rats in the CP + API group were given a single dosage of 7.5 mg/kg/day CP and then 0.5 g/kg/day API. Our research application caused zero animal loss. To decapitate the animals under general anesthesia at the finish of the experiment, intraperitoneal injections of ketamine (50 mg/kg body weight; Ketalar flacon; Pfizer, New York, USA) and xylazine (10 mg/kg body weight; Rompun; Bayer, Leverkusen, Germany) were administered. The tissues of the right and left ovary were removed. The right ovary was preserved in 10 % formaldehyde for histological and immunohistochemical analysis, while the left ovary was kept at −80 °C for biochemical research.

2.3. Ovarian morphology evaluation

The tissues were dehydrated using increasingly higher alcohols following their formalin fixation, xylene rinsing, and paraffin embedding. After cutting and mounting on a slide, the serial section with a thickness of 5 μm was obtained. Following being deparaffinized with xylene, sections were rehydrated and stained with either Masson trichrome or Hematoxylin and eosin (H&E) to evaluate the histology (Yalçın et al., 2024). Using an Olympus BX51 microscope (Tokyo, Japan) equipped with a DP-71 camera, sections have been examined and photographed on camera. Ovarian tissue damage was evaluated in terms of congested blood vessels (Ayazoglu Demir et al., 2022), vacuolization, and edema (Mete Ural et al., 2016). The assessment was graded semi-quantitatively for each criterion from 0 to 3 (0: none, 1: mild, 2: moderate, 3: severe).

2.4. Follicle morphological classification and counting

At the moment the ovarian tissue began to emerge on the paraffin block, 10 consecutive sections were obtained. 10 parts were eliminated. The entire ovary was scanned while this cycle was repeated. 1., 5., and 10 of the ten sections that were removed for assessment were divided up for hematoxylin-eosin staining and follicle counting. Follicle counting was carried out on serial sections of ovarian tissue that were taken from each study group. The follicles were carefully categorized by two histologists using the primordial, primary, preantral, antral, and atretic categories. Follicles are classified morphologically according to the number of layers and the form of the granulosa cells. A complete basal lamina, an oocyte, a germinal vesicle, and a complete nucleolus were all present in healthy follicles. Died granulosa cells and pyknotic nuclei revealed follicles that showed signs of damage (Onder et al., 2021).

2.5. Immunohistochemistry

The immunohistochemical staining kit (Lab VisionTM Ultra-VisionTM Large Volume Detection System: anti-polyvalent, HRP, TA-125-HL) was used in conjunction with the streptavidin-biotin-peroxidase method. This method was used to identify the expressions of Beclin-1, p62, LC3-2, Caspase-3, and apoptosis-inducing factor (AIF) in ovarian tissues. Five micron-thick cross-sections of ovarian tissue blocks were cut, deparaffinized, rehydrated, and then washed at room temperature in phosphate-buffered saline (PBS). To prevent endogenous peroxidase activity, 3 % hydrogen peroxide was applied for 5 min. They were rewashed with PBS and then allowed to recover antigens in 10 % sodium citrate buffer (pH 6.0) for 5 min at 95 °C in the microwave oven. They were subsequently allowed to rest at room temperature for a total of 20 min. Primary antibodies Beclin-1 (Novus, NB500-249; 1:200), p62 (Anti-SQSTM-1, H00008878; 1:200), LC-3 (Cell Signaling, 12741S; 1:500), Caspase-3 (Cell Signaling Technology, Leiden, Netherlands; 1:500), and apoptosis-inducing factor (Bioss, bs-1363R; 1:400) were treated with the sections for an entire night at 4 °C. The sections were treated with biotinylated secondary antibodies. After washing, apply the streptavidin peroxidase complex and utilize 3,3′-*p*-diaminobenzidine

tetrahydrochloride chromogen. Mayer's hematoxylin was applied to counterstain it. For each part of the ovaries, images were captured from 10 separate locations using a digital camera (DP71) set on an Olympus BX51 light microscope (Tokyo, Japan). Using the Image J software program (Jensen, 2013; Schindelin et al., 2012)(NIH; Washington, U.S. A.), immunoreactivity densities of Beclin-1, p62, LC3-2, Caspase-3, and apoptosis-inducing factor (AIF) were determined.

2.6. Examination of the levels of malondialdehyde (MDA), glutathione peroxidase (GSH-Px), superoxide dismutase (SOD), and catalase (CAT) in tissue

Ovary tissues that had been frozen were blended with PBS (0.01 M, pH 7.4), homogenized, and centrifuged for 10 min at 4 °C at 3000 rpm. For the ELISA procedure, the obtained supernatant was divided into portions. We measured MDA, GSH-Px, SOD, and CAT. Sunred Biological Technology Co. examined the supernatant at 450 nm using a Thermo Fisher Scientific microplate reader and a brand advertising kit. In order MDA (Rat malondialdehite Sunred Biological Technology 201-11-0157), GSH-Px (Rat GSH-PX Sunred Biological Technology 201-11-5104), SOD (Rat Superoxide dismutase Sunred Biological Technology 201-11-0169), and CAT (Rat Catalase Sunred Biological Technology 201-11-5106) were used in enzyme-linked immunosorbent test protocols.

2.7. AMH, FSH, and LH level measurement

Following the experiment, the animals were executed by dislocating their cervical vertebral bodies, and the blood was gathered in biochemical tubes. After 10-min centrifugation at 3000 rpm to separate serum, blood samples were stored at 80 °C until the levels of AMH (Rat Anti Mullerian Hormone ELISA kit 201-11-1246), FSH (Rat follicle-stimulating hormone ELISA Kit 201-11-0183) and LH (Rat luteotropic hormone ELISA Kit 201-11-0180) were determined. Sunred Biological Technology Co., Ltd. of the brand kit examined the supernatant at 450 nm using a microplate reader (Thermo Fisher Scientific) to determine the therapeutic value of these hormones in the serum.

2.8. Statistical analysis

Graphpad Prism Version 9 was used for all statistical analyses. The data distributed was determined by the Shapiro-Wilk test. The Kruskal-Wallis test and one-way analysis of variance (ANOVA) were utilized for comparisons combining more than two groups. Significant post-hoc comparisons of the variables were shown by the Dunn test for the Kruskal-Wallis analysis and the Bonferroni test for the one-way ANOVA test. The results of the p below 0.05 were regarded as statistically important for all data.

3. Results

3.1. Histopathological findings of the ovary

Fig. 1 demonstrates the findings of a rat ovarian tissue histological investigation. Ovarian tissues from both the Control and API groups were examined under a microscope and demonstrated a normal histological architecture with all types of follicles. In the control groups, follicles were normal at various stages, with oocytes centrally positioned and surrounded by directed granulosa cells. The medullary area comprises loose connective tissue and has a healthy vascular network. In the CP group, the histological architecture deteriorates and the growth of ovarian series follicles is regressed. In addition, the CP group reported congested blood vessel, vacuolization, and ovarian tissue edema. The CP group had a significantly higher rate of congested blood vessel ($p < 0.001$), vacuolization ($p < 0.001$), and edema ($p < 0.001$) than the control group. API therapy alleviated congested blood vessel ($p > 0.05$), vacuolization ($p < 0.05$), and edema ($p > 0.05$), while also promoting healthy follicle growth in the CP + API group (Fig. 2). The total number of primitives, primary, preantral, secondary Graafian, and Atretic follicles in all groups was counted (Table 1). The number of malformed, or atretic, follicles was higher in the CP group, but this distinction was not statistically significant. The number of primordial follicles in this group showed a statistically significant decrease compared to the control group ($p < 0.01$). Although API therapy reduces the number of atretic follicles in the CP + API group, the number of primordial, preantral, and secondary follicles developing was higher in this group (Table 1). In our

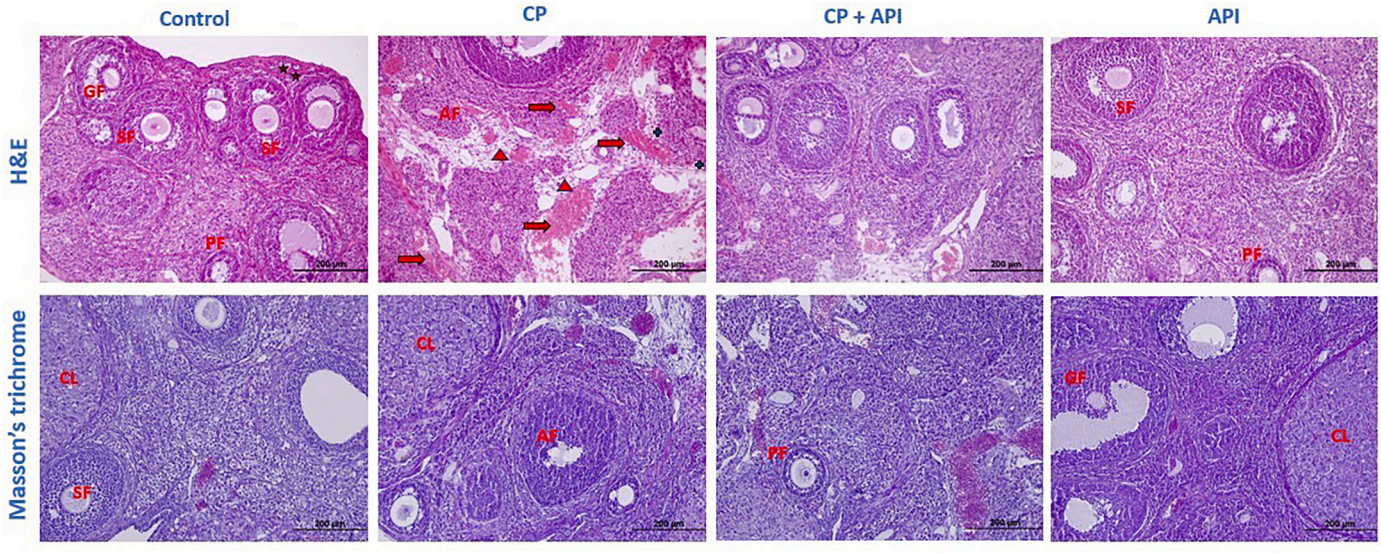

Fig. 1. Light microscopic findings in the rat ovary tissue. Control group: Several developmental phases of folliculi are found. CP group: at various stages of development, there were noticeably fewer follicles. CP+API group: a considerable number of follicles in different growth phases are detected in this group compared to the CP group. Primordial follicles (*), primary follicles (PF), the secondary follicle (SF), and Corpora lutea (CL) with large, weakly pigmented acidophilic cells, mature Graafan follicle (GF), and atretic follicles (AF). Congested blood vessels (thin red arrow), vacuolization (red arrowhead), and edema (+). H&E: hematoxylin-eosin and Masson's trichrome staining (Olympus BX51, Tokyo, Japan. X20). (For interpretation of the references to colour in this figure legend, the reader is referred to the web version of this article.)

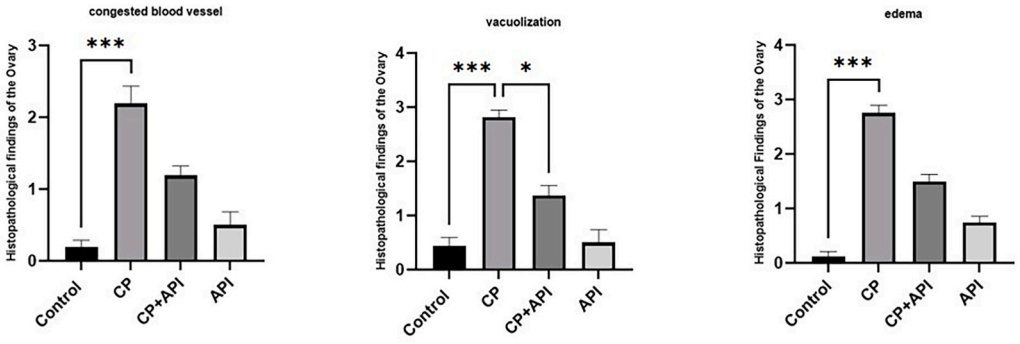

Ovary Histoscore	Control	CP	CP + API	API	P
Congested blood vessel	0.000(0.000-1.000)	2.500(0.000-3.000)	1.000(0.000-2.000)	0.000(0.000-2.000)	<.001
vacuolization	0.000(0.000-2.000)	3.000(1.000-3.000)	1.000(1.000-3.000)	0.000(0.000-3.000)	<.001
edema	0.000(0.000-1.000)	3.000(1.000-3.000)	1.500(1.000-2.000)	1.000(0.000-1.000)	<.001

Fig. 2. Congested blood vessels, vacuolization, and edema ovary histoscore in the experimental groups. Data were presented as mean ± standard deviation and median (min-max). *: $p < 0.05$, **: $p < 0.01$, ***: $p < 0.001$.

Table 1
Follicle scores in the experimental groups. Data were presented as mean ± standard deviation and median (min-max). *: $p < 0.05$, **: $p < 0.01$, ***: $p < 0.001$. **Primordial follicles**: **Control and CP group.

Follicle Score	Control (n = 7)	CP (n = 7)	CP + API (n = 7)	API (n = 7)	p
Primordial follicle	7.429 ± 3.409	2.143 ± 1.574	4.571 ± 2.573	5.000 ± 1.915	0.006
Primer follicle	4.714 ± 1.604	3.000 ± 2.646	2.143 ± 0.6901	2.714 ± 1.799	0.077
Preantral follicle	4.000 (1.000–5.000)	1.000 (1.000–4.000)	2.000 (2.000–4.000)	3.000 (1.000–5.000)	0.287
Seconder follicle	5.000 (0.000–6.000)	1.000 (0.000–5.000)	5.000 (0.000–6.000)	3.000 (1.000–4.000)	0.050
Graffian follicle	0.000 (0.000–2.000)	1.000 (0.000–1.000)	0.000 (0.000–3.000)	1.000 (0.000–2.000)	0.939
Atretic follicle	1.000 (0.000–5.000)	5.000 (2.000–6.000)	4.000 (2.000–5.000)	3.000 (2.000–4.000)	0.007

study, we used the Masson trichome method to assess the overall appearance of the ovarian connective tissue stroma in all experimental groups. There was no significant difference between the groups in terms of connective tissue or collagen fiber density. (Fig. 1).

3.2. Autophagy markers

Beclin-1, p62, and LC3 positive cells were assessed independently for each group, and correlations were made between groups. Beclin-1 reactivity in the granulosa cells of the follicles and the ovarian stroma. Granulosa cells showed positivity for P62 and LC-3 within the cytoplasm. The CP group had a slightly higher level of Beclin-1 immunoreactivity density than the control group. The increase did not reach statistical significance ($p > 0.05$). In the CP + API group, API therapy reduced Beclin-1 expression. Additionally, the Beclin-1 expression in the API group was similar to the control group (Fig. 3 and Table 2).

One of the autophagy markers, P62, showed a statistically significant boost in the CP group ($p < 0.01$). The API therapy declined the P62 immunoreactivity density in the CP + API group ($p < 0.01$) (Fig. 3 and Table 2). P62 expression improved only in the API group compared to the control group, but it the difference was statistically insignificant ($p > 0.05$).

LC-3 expression increased substantially in the CP group compared to the control group ($p < 0.05$). API therapy did not reduce LC-3 expression in the CP + API group. Moreover, LC-3 expression showed a statistically significant increase in the API group compared to the control group ($p < 0.001$) (Fig. 3 and Table 2).

3.3. Apoptosis markers

All experimental groups ovary tissue was analyzed for the expression level of Caspase-3 and AIF, the two apoptosis markers. These markers were positively detected in germinal epithelial cells, follicular granulosa cells, ovarian stroma, and the corpus luteum. Caspase-3 immunoreactivity was higher in the CP group ovary than in the control group. API treatment in the CP + API group reduced Caspase-3 immunoreactivity. These results were not statistically significant ($p > 0.05$). The density of Caspase-3 immunoreactivity in the API group was statistically significantly higher than in the CP + API group ($p < 0.05$) (Fig. 4 and Table 2).

AIF expression increased significantly in the CP group compared to the control group, indicating increased apoptosis ($p < 0.001$). AIF expression in the API group increased significantly as compared to the control ($p < 0.001$) and CP + API groups ($p < 0.01$) (Fig. 4 and Table 2).

3.4. Lipid peroxidation level and antioxidant indicate

MDA is a lipid peroxidation product. The CP group had higher levels of MDA ovary tissue than the control group ($p > 0.05$). The CP + API group exhibited decreased MDA ovary tissue levels than the CP group ($p > 0.05$). In comparison to the control group, the tissue MDA level in the API group increased and approximated that of the CP group ($p > 0.05$) (Fig. 5 and Table 3).

The GSH-PX levels in the ovarian tissue of the CP group were lower compared to those in the control group ($p < 0.01$). API therapy didn't improve restore tissue GSH-PX levels in the CP + API group. However, in

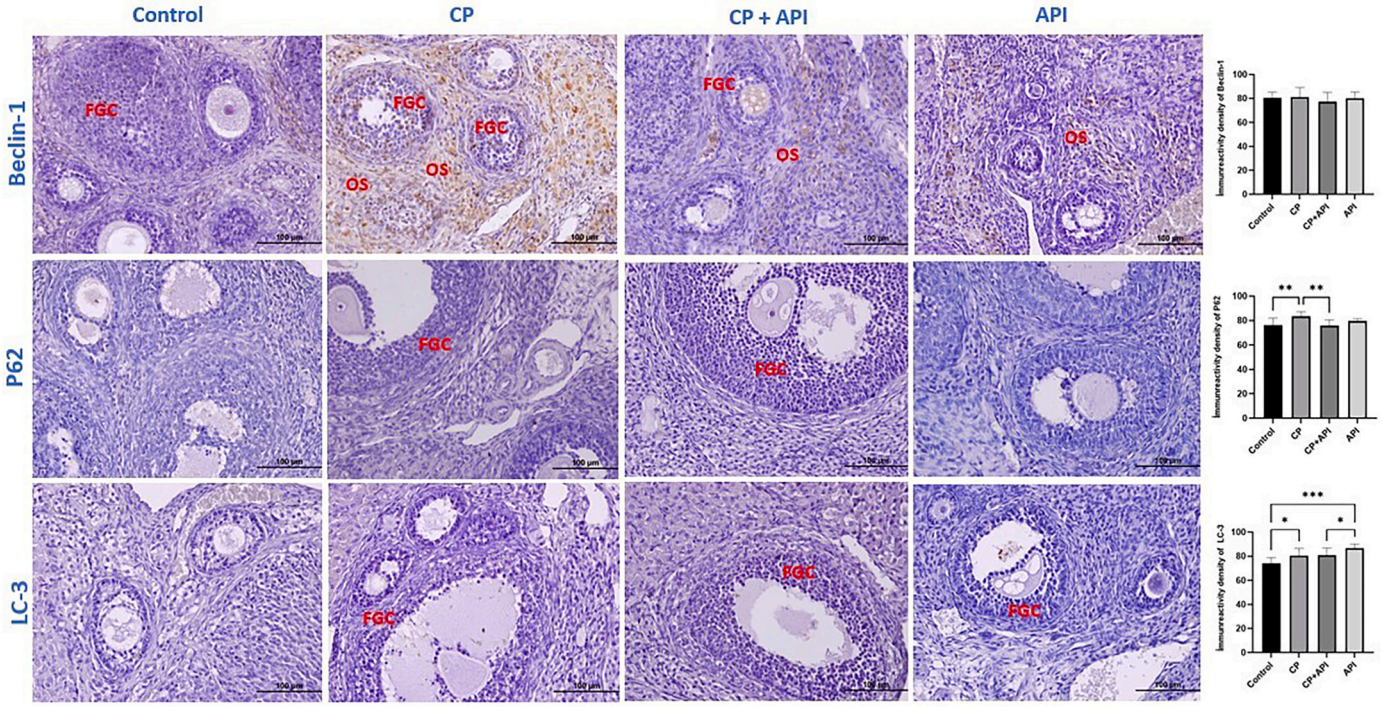

Fig. 3. Immunohistochemical microscopic findings and graphics. Expressions of autophagy markers Beclin-1, p62, and LC-3 in ovarian tissue of all experimental groups. *: $p < 0.05$, **: $p < 0.01$, ***: $p < 0.001$. Follicular granulosa cells (FGC) and Ovarian stroma (OS) (Olympus BX51, Tokyo, Japan. X20).

Table 2
In the experimental group, the immunoreactivity density of autophagy markers Beclin-1, P-62, and LC-3 levels and apoptosis markers Caspase-3 and AIF. Data were presented as mean ± standard deviation and median (min-max). *: $p < 0.05$, **: $p < 0.01$, ***: $p < 0.001$. **P62**: **Control and CP group, **CP and CP + API group. **LC-3**: *Control and CP group, ***Control and API group, *CP + API and API group. **Caspase-3**: *CP + API and API group. **AIF**: ***Control and CP group, ***Control and API group, **CP + API and API group.

IHC Marker	Control (n = 7)	CP (n = 7)	CP + API (n = 7)	API (n = 7)	p
Autophagy Marker					
Beclin-1	79.82 (71.16–89.00)	80.80 (66.12–93.07)	75.41 (64.61–88.39)	79.87 (71.77–92.84)	0.297
P62	74.28 (70.97–88.73)	83.07 (77.89–89.20)	76.25 (67.50–84.87)	79.52 (75.77–81.95)	0.002
LC-3	72.97 (65.89–83.22)	80.36 (72.21–98.42)	80.55 (72.59–95.67)	89.93 (83.09–89.93)	<0.001
Apoptosis Marker					
Caspase-3	80.47 (75.07–90.89)	82.94 (70.88–86.63)	81.92 (75.66–100.0)	86.40 (81.96–93.60)	0.019
AIF	79.23 (69.70–88.84)	83.79 (73.26–98.98)	81.98 (74.49–94.16)	87.36(72.49–96.35)	<0.001

the API group, the tissue GSH-PX level was statistically significantly lower than in the control group ($p < 0.01$) (Fig. 5 and Table 3).

When the tissue SOD levels were examined between the experimental groups, it emerged that the CP group had a lower level than the control group ($p > 0.05$). API therapy administered to the CP + API group, improved this level. This increase was statistically significant ($p < 0.05$). In the API group SOD tissue antioxidant levels were lower than the control group, as was the GSH-PX indicator ($p > 0.05$) (Fig. 5 and Table 3).

Tissue CAT levels declined in the CP group compared to the control group ($p > 0.05$). However, API treatment boosted this level in the CP + API group($p < 0.01$) (Fig. 5 and Table 3).

3.5. Hormone levels

The CP group had a substantially lower blood AMH level than the control group($p < 0.01$). However, after API treatment, the level improved in the CP + API group than in the CP group ($p > 0.05$). Still, the API group exhibited lower AMH levels than the control group. (Fig. 6 and Table 3).

The serum FSH level diminished in the CP group compared to the control group ($p > 0.05$). However, following API therapy, the levels increased in the CP + API group compared to the CP group ($p > 0.05$) (Fig. 6 and Table 3).

Unlike other hormones, LH serum levels were not reduced in the CP group as compared to the control group. It remained at approximately the same levels. The LH level decreased slightly in the API group compared to the control (Fig. 6 and Table 3).

4. Discussion

One of the most well-known anticancer medications CP is used to treat several cancers, such as ovarian, bladder, testicular, head and neck, and esophageal cancers (Zoń and Bednarek, 2023). The negative consequences of anticancer drugs used in chemotherapy, a popular cancer treatment strategy, on normal cells and tissues, continue to be a problem that must be resolved (Zhang et al., 2018). Chemotherapy alters physiological balance and can harm multiple organs during treatment (Rafiee et al., 2020). Chemotherapeutics are the leading cause of ovarian damage. Preventing primordial follicle loss and premature ovarian aging will benefit children, adolescents, and young women with reproductive potential. Primordial follicles are extremely vulnerable to radiotherapy and chemotherapy. During chemotherapy, follicular reserve declines and rapid aging happens (Dayangan Sayan et al., 2018). In this regard,

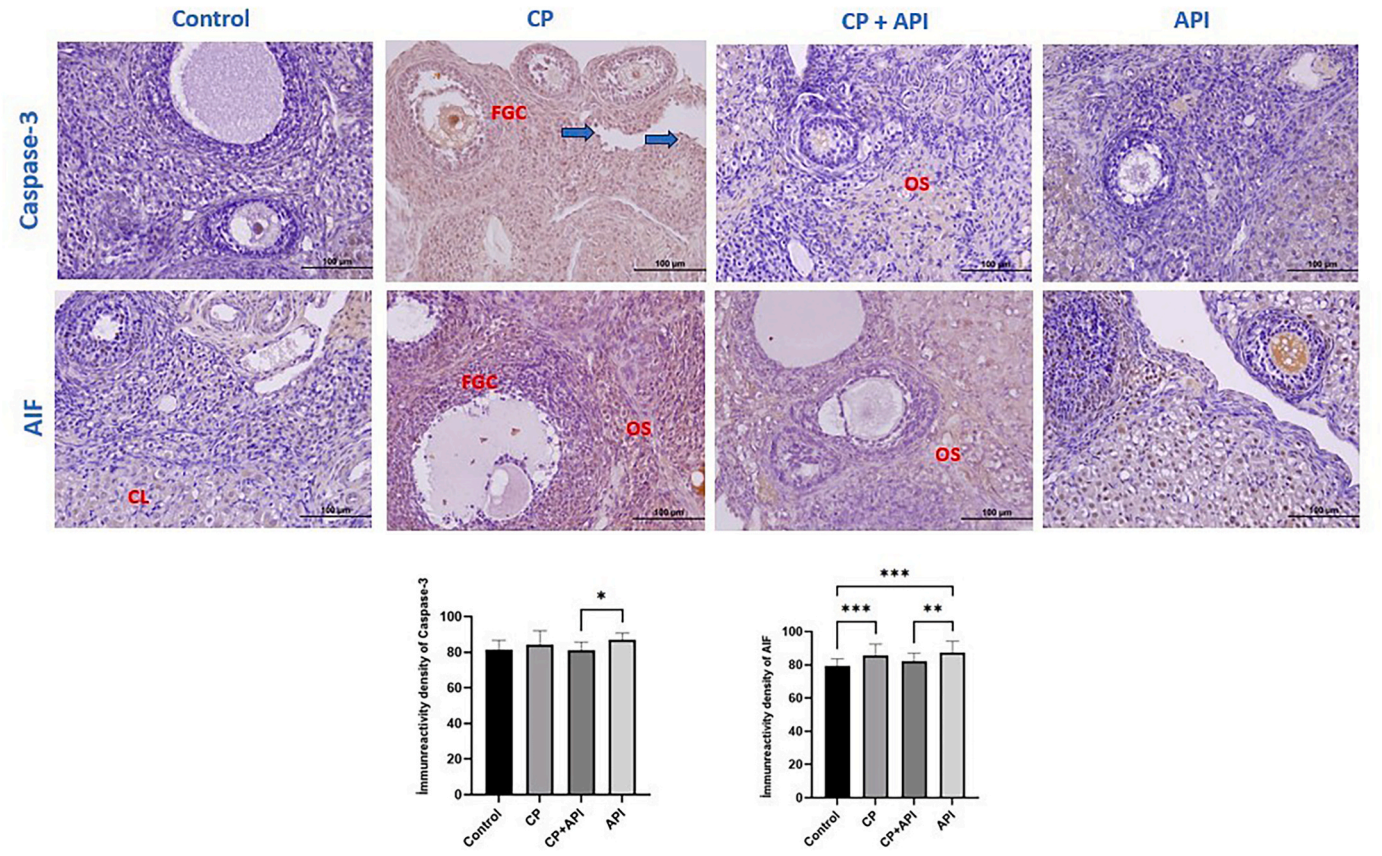

Fig. 4. Immunohistochemical microscopic findings and graphics. Expressions of apoptosis markers Caspase-3 and AIF in ovarian tissue of all experimental groups. *: $p < 0.05$, **: $p < 0.01$, ***: $p < 0.001$. Follicular granulosa cells (FGC), Corpora lutea (CL), Ovarian stroma (OS), and Germinal epithelial cells (thin blue arrow) (Olympus BX51, Tokyo, Japan. X20). (For interpretation of the references to colour in this figure legend, the reader is referred to the web version of this article.)

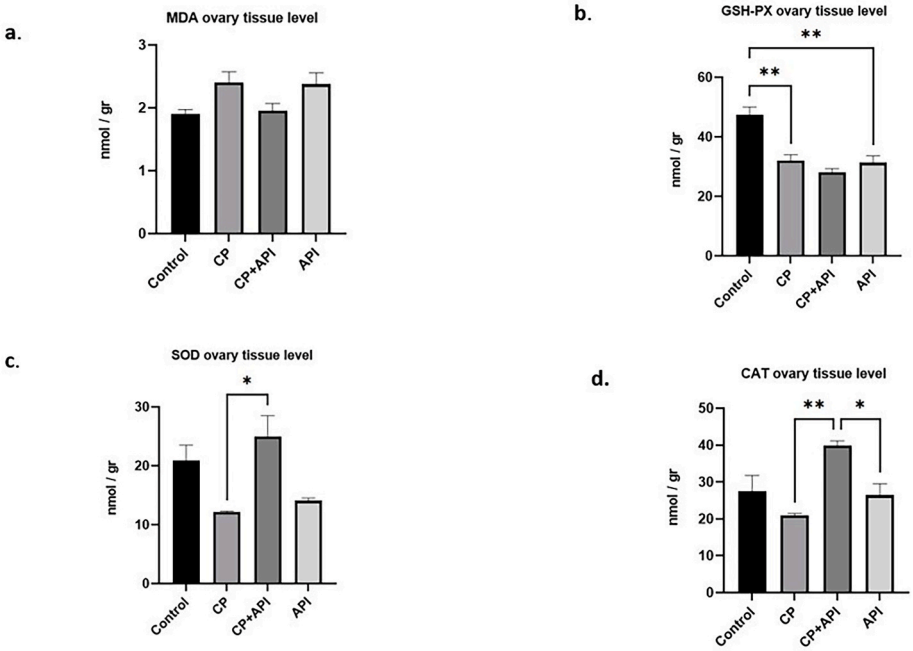

Fig. 5. A statistical analysis of the experimental groups' serum levels of MDA, GSH-PX, SOD, and CAT, expressed graphically. *: $p < 0.05$, **: $p < 0.01$, ***: $p < 0.001$.

Table 3
Levels of lipid peroxidation product MDA and antioxidant enzymes GSH-PX, SOD, and CAT in the serum of the experimental groups. Also AMH, FSH, and LH hormone levels. Data were presented as mean ± standard deviation and median (min-max). *: $p < 0.05$, **: $p < 0.01$, ***: $p < 0.001$. **GSH-PX**: **Control and CP group, **Control and API group. **SOD**: *CP and CP + API group. **CAT**: **CP and CP + API, *CP + API and API group. **AMH**: **Control and CP group, **Control and CP + API, *Control and API group.

ELISA products	Control (n = 7)	CP (n = 7)	CP + API (n = 7)	API (n = 7)	p
Lipid peroxidation					
MDA	1.900 ± 0.1272	2.407 ± 0.2899	1.954 ± 0.1983	2.375 ± 0.3155	0.064
Antioxidant status					
GSH-PX	47.36 ± 4.587	32.04 ± 3.334	28.00 ± 2.315	31.29 ± 3.980	<0.001
SOD	20.86 ± 4.596	12.13 ± 0.3200	24.98 ± 6.100	14.08 ± 0.8125	0.011
CAT	27.52 ± 7.379	20.96 ± 0.9120	39.94 ± 2.131	26.46 ± 5.412	0.007
Hormone status					
AMH	2516.0 ± 641.8	303.1 ± 193.3	673.9 ± 470.5	1180.0 ± 362.5	0.002
FSH	20.57 ± 5.865	15.31 ± 2.854	16.42 ± 15.76	13.60 ± 4.260	0.796
LH	26.55 ± 7.072	26.48 ± 11.31	26.82 ± 2.888	24.79 ± 3.464	0.983

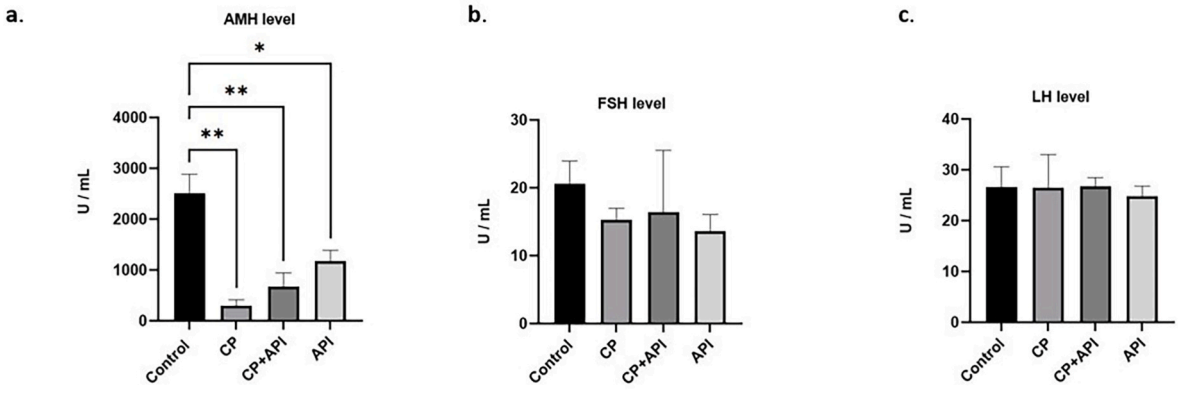

Fig. 6. A statistical analysis of the experimental groups' AMH, FSH, and LH hormone levels expressed graphically. *: $p < 0.05$, **: $p < 0.01$, ***: $p < 0.001$.

CP significantly lowers the number of primordial follicles in the ovary, according to recent research aiming to restore the ovarian reserve (Mentese et al., 2022; Sakin et al., 2020). Another recent study on rats found that CP led to ovarian harm. As a result of this harm, the CP group's number of primordial follicles declined relative to the control group (Ayazoglu Demir et al., 2023). We found that CP damaged ovarian tissue and reduced the number of primordial follicles in the CP group, which is in line with these results. Exposure to CP resulted in histopathologic alterations in ovarian tissue in an additional study. These alterations included congestion in blood vessels and edema in the ovarian stroma (Anğın et al., 2020). In ovarian tissue treated with CP, a group of investigators discovered edema, hemorrhage, and dilated congestive blood vessels (Kulhan et al., 2019). Our research is on the findings that show these histopathologic abnormalities. According to research, many of the autophagy molecules and signaling pathways involved in the autophagy process are linked to apoptosis (Xi et al., 2022). As a result, we examined apoptosis and autophagy indicators by immunohistochemistry. In a cell culture study conducted using a different approach, Beclin-1, an autophagy marker, climbed in the CP damage group compared to the control group, but P62 levels declined (Xu et al., 2024). In another study, ovarian damage was caused by a different method, and autophagy markers were evaluated. In this study, Beclin-1, P62, and LC-3 expression levels were elevated in the ovarian damage group, which is consistent with what we found (Karaman et al., 2024).

Oxidative stress is caused by an alteration in the balance between the production of reactive oxygen species (ROS) and the mechanism of antioxidant defense. This imbalance creates a variety of tissue damage and is the fundamental cause of many diseases and pathological circumstances. Both exogenous (such as ultraviolet rays, nicotine, pollutants from the environment, heavy metals, and drugs) and endogenous (such as mitochondrial respiration, cytochrome P450 enzymes, neutrophils, and macrophages involved in inflammation) factors may result in oxidative stress (Hajam et al., 2022). CP-induced oxidative stress is known to cause cell death via apoptosis. Apoptosis reduces the number and growth of ovarian follicles, resulting in atresia before ovulation. Research suggests that CP-induced apoptosis activates AIF and Caspase-3 are commonly used biomarkers for assessing apoptosis in tissue (Altındağ and Meydan, 2021; Zoń and Bednarek, 2023) In another investigation, Caspase-3 levels increased in the CP group, demonstrating that CP induces apoptosis in ovarian tissue (Ayazoglu Demir et al., 2023). In the ovarian ischemia-reperfusion model, the enhanced reactivity of Caspase-3 and AIF markers in the damage groups was consistent with what we found (Karakus and Ozkaraca, 2024). Furthermore, our findings confirm our follicle count results, which showed larger follicular degeneration, particularly in the CP group. As it deals with cellular oxidative stress, CP can suppress the activity of antioxidant enzymes including GSH-Px, CAT, and SOD, while simultaneously increasing oxidative stress in tissues (Malik et al., 2015). MDA is widely recognized as the main byproduct of membrane lipid peroxidation. Our findings align with recent studies, and the CP group's tissue MDA level increased, and antioxidant levels decreased (Du et al., 2023; Ibrahim et al., 2021). Steroidogenesis is the more complex chain of processes that occur during the synthesis and secretion of sex steroid hormones from ovarian cells (Fletcher et al., 2022). Consequently, we examined the fate of FSH and LH hormone levels in the CP group. Although our findings disagreed with the literature, these hormones were lower in the CP group compared to the control group (Al-Shahat et al., 2022; Cheng et al., 2020; Hashem et al., 2020; Ibrahim et al., 2021). Serum AMH concentration, an effective marker of ovarian damage and reserve, falls with follicular destruction. The findings we obtained demonstrated that serum AMH levels in the CP group were significantly lower than in the control group, expected given the detrimental effects of CP (Said et al., 2019). Apitherapy, the science of employing bee products, has advanced

rapidly because current treatment approaches are insufficient to eliminate existing health problems and have side effects that lower quality of life (Weis et al., 2022). The most well-known products used in apitherapy are honey, pollen, propolis, bee bread, and royal jelly, which have multiple biological and medicinal applications (Özdemir et al., 2021). In recent years, drone larvae; API is also rich in vital components, enhancing the chances of its use in apitherapy as therapeutic support (Topal et al., 2018). The realized agents' preventive and therapeutic effects on the male and female genital systems are well established (Fratellone et al., 2016). API is a bee product consisting of androgens and provides on both male and female reproductive glands (Silici, 2023). However, API therapy for CP-induced ovarian impairment has not been explored. Hashem et al. investigated the probable value of royal jelly against CP-induced ovarian damage revealing that it pushed the number of developing follicles, fell the number of atretic follicles, and corrected the harmed histological architecture indicated in the CP group (Hashem et al., 2020). In one of the studies of bee products to alleviate ovary-related damage, microscopic findings from HE staining in a rat model of ovarian failure reveal that % 50 honey bee products enhance ovarian regeneration by minimizing hemorrhage and congestion (Safitri et al., 2016). In a letrozole-induced PCOS model, Sapmaz et al. observed that 50 mg/kg of propolis boosted the number of cystic follicles (Sapmaz et al., 2022). In line with all of previous investigations, API therapy considerably reduced the congested blood vessels, vacuolization, and edema produced by CP in ovarian tissue in our study. The API application was able to get the values closer to healthy levels. In other words, it reduced the number of atretic follicles while increasing the number of primordial follicles. In line with the positive therapeutic results obtained from API treatment, Koç et al. investigated the influence of propolis on ischemia-reperfusion injury in the ovary and discovered that it reduced Caspase −3 Immunoreactivity (Koc et al., 2019). The expression of this marker in CP-induced ovarian damage was only slightly decreased by API treatment, which was less than we were expecting. This finding indicates that API may control apoptotic processes and lower Caspase-3 levels, yet its effectiveness is limited. In a novel study, activation of AIF and caspase-3 genes, which are proapoptotic markers, increased ovarian exposure to postnatal chromium(VI), an endocrine disruptor in rats. However, there is no research in the literature on an API to reduce this rise in AIF (Dutta et al., 2024). Our findings demonstrated that API had the potential to attenuate CP-induced apoptosis. Beclin-1, P62, and LC3 are key molecules in the autophagy process. Beclin-1 plays a key function in the beginning stages of the autophagy process. Increased Beclin-1 expression usually implies that autophagy is active. P62 is an autophagy substrate that helps mark cellular material for autophagic destruction. LC3 is a marker for the onset of autophagic vesicles (autophagosomes)(Mundo Rivera et al., 2024). Relating the implications of bee products on autophagy in ovarian damage, there was no information available regarding the expression of autophagy markers. Yet the latest study has used several supplements to improve ovarian function and minimize autophagy (Karaman et al., 2024; Miao et al., 2023). According to our research, API therapy lowered Beclin-1 and particularly P62 immunoreactivity, which had risen in the CP group. On the other hand, it failed to reduce LC-3 immunoreactivity, which was also elevated in the CP group. Apilarnil improved CP-induced autophagic and apoptotic processes by diminishing Beclin-1 and P62 levels. However, the absence of effect on LC3 levels shows that API is only effective at particular phases of the autophagy process. A different approach PCOS study reported that honey bee venom reduced the elevated AMH level in the PCOS model, contradicting current AMH level findings (Pouyanmanesh et al., 2013). In our current study, API increased the lowering AMH level. Although API has a protective impact, alternative therapies may be required to fully restore ovarian reserve, given its effectiveness on follicle counts. A study looked at FSH and LH levels in cadmium-induced ovarian injury, and the results were similar to ours as well. In this study, Tualang honey enhanced the results (Ruslee et al., 2020). In our investigation, API therapy slightly elevated FSH levels but did not significantly alter LH levels. The preventive and therapeutic potential of Apilarnil (API) on these significant mechanisms was assessed in this investigation, which also examined important mechanisms like oxidative stress, autophagy, and apoptosis brought on by CP treatment in ovarian tissue. Histopathological and biochemical analyses revealed that API therapy improved ovarian reserve and reduced CP-induced ovarian damage. According to study findings, apitherapy products like API can lessen the toxicity of CP in ovarian tissue.

5. Conclusion

In this study, we focused into the effect of CP on the ovary in the female reproductive system. We hypothesized that API, a naturally existing molecule, might exert a therapeutic effect on this negative consequence. After evaluating the histological, immunohistochemical, and biochemical findings, we concluded that API was efficient for decreasing CP-induced ovarian damage. API improved autophagic processes by lessening the levels of Beclin-1 and P62, as well as oxidative stress-induced apoptotic markers including Caspase-3 and AIF. However, API's not much impact on LC3 expression shows that autophagic circulation is not completely regulated. The primary limitation of this study is the use of a fixed dose of API (0.5 g/kg) administered over a 10-day period, which may not reflect the full range of potential dose-dependent effects. Additionally, the lack of a more detailed investigation into autophagic processes represents another significant limitation. The findings of this study indicate that API, an organic compound used in apitherapy, may protect the ovary from damage induced by CP treatment. However, more comprehensive and prolonged studies are needed to refine its effectiveness and fully uncover its mechanisms of action. To evaluate the absence of components of API on the autophagy process, the molecular processes that explain their actions should be researched.

CRediT authorship contribution statement

Kübra Tuğçe Kalkan: Writing – review & editing, Writing – original draft, Validation, Project administration, Methodology, Investigation. **Halime Tozak Yıldız:** Methodology, Investigation. **Betül Yalçın:** Methodology, Formal analysis. **Özge Cengiz Mat:** Validation, Investigation. **Gözde Özge Önder:** Validation, Conceptualization. **Arzu Yay:** Visualization, Investigation, Funding acquisition, Conceptualization.

Funding

It received support from Kırşehir Ahi Evran University Scientific Research Unit as project number TIP.A2.24.001.

Data availability statement

The data used to support the findings of this study are included in the article.

Declaration of competing interest

The authors declare that they have no known competing financial interests or personal relationships that could have appeared to influence the work reported in this paper.

Acknowledgements

We would like to thank the Erciyes University (ERU) Experimental Research and Application Unit staff for caring for the rats used in this investigation.

Data availability

Data will be made available on request.

References

Aboraya, D.M., El Baz, A., Risha, E.F., Abdelhamid, F.M., 2022. Hesperidin ameliorates cisplatin induced hepatotoxicity and attenuates oxidative damage, cell apoptosis, and inflammation in rats. Saudi J. Biol. Sci. 29, 3157–3166. https://doi.org/10.1016/j.sjbs.2022.01.052.

Al-Shahat, A., Hulail, M.A., Soliman, N.M., Khamis, T., Fericean, L.M., Arisha, A.H., Moawad, R.S., 2022. Melatonin mitigates cisplatin-induced ovarian dysfunction via altering steroidogenesis, inflammation, apoptosis, oxidative stress, and PTEN/PI3K/Akt/mTOR/AMPK signaling pathway in female rats. Pharmaceutics 14, 2769. https://doi.org/10.3390/pharmaceutics14122769.

Altındağ, F., Meydan, İ., 2021. Evaluation of protective effects of gallic acid on cisplatin-induced testicular and epididymal damage. Andrologia 53, e14189. https://doi.org/10.1111/and.14189.

Anğın, A.D., Gün, I., Sakin, Ö., Çıkman, M.S., Şimşek, E.E., Karakuş, R., Başak, K., Kaptanağası, A.O., 2020. Investigation of the preventive effects of dehydroepiandrosterone (DHEA) and Caffeic acid phenethyl ester (CAPE) on cisplatin-induced ovarian damage in rats. Ultrastruct. Pathol. 44, 71–80. https://doi.org/10.1080/01913123.2019.1711479.

Ashcroft, R.E., 2008. The declaration of Helsinki. The Oxford Textbook of Clinical Research Ethics, pp. 141–148. https://doi.org/10.1093/med/9780195168655.001.0001.

Atli, M., Engin-Ustun, Y., Tokmak, A., Caydere, M., Hucumenoglu, S., Topcuoglu, C., 2017. Dose dependent effect of resveratrol in preventing cisplatin-induced ovarian damage in rats: an experimental study. Reprod. Biol. 17, 274–280. https://doi.org/10.1016/j.repbio.2017.07.001.

Ayazoglu Demir, E., Mentese, A., Kucuk, H., Turkmen Alemdar, N., Demir, S., 2022. p-Coumaric acid alleviates cisplatin-induced ovarian toxicity in rats. J. Obstet. Gynaecol. Res. 48, 411–419. https://doi.org/10.1111/jog.15119.

Ayazoglu Demir, E., Mentese, A., Livaoglu, A., Turkmen Alemdar, N., Demir, S., 2023. Ameliorative effect of gallic acid on cisplatin-induced ovarian toxicity in rats. Drug Chem. Toxicol. 46, 97–103. https://doi.org/10.1080/01480545.2021.2011312.

Babacan, A.A., Ayar, A., 2024. Effects of apilarnil and queen bee larvae on larval mortality and longevity in *Drosophila melanogaster*. Uludag Bee J. 24, 223–234. https://doi.org/10.31467/uluaricilik.1494204.

Bortnik, S., Gorski, S.M., 2017. Clinical applications of autophagy proteins in cancer: from potential targets to biomarkers. Int. J. Mol. Sci. 18, 1496. https://doi.org/10.3390/ijms18071496.

Cheng, J.-C., Fang, L., Li, Y., Wang, S., Li, Y., Yan, Y., Jia, Q., Wu, Z., Wang, Z., Han, X., 2020. Melatonin stimulates aromatase expression and estradiol production in human granulosa-lutein cells: relevance for high serum estradiol levels in patients with ovarian hyperstimulation syndrome. Exp. Mol. Med. 52, 1341–1350. https://doi.org/10.1038/s12276-020-00491-w.

Dayangan Sayan, C., Tulmac, O.B., Karaca, G., Ozkan, Z.S., Yalcin, S., Devrim, T., Dindar Badem, N., 2018. Could erythropoietin reduce the ovarian damage of cisplatin in female rats? Gynecol. Endocrinol. 34, 309–313. https://doi.org/10.1080/09513590.2017.1395836.

Du, R., Cheng, X., Ji, J., Lu, Y., Xie, Y., Wang, W., Xu, Y., Zhang, Y., 2023. Mechanism of ferroptosis in a rat model of premature ovarian insufficiency induced by cisplatin. Sci. Rep. 13, 4463. https://doi.org/10.1038/s41598-023-31712-7.

Dutta, S., Sivakumar, K.K., Erwin, J.W., Stanley, J.A., Arosh, J.A., Taylor, R.J., Banu, S. K., 2024. Alteration of epigenetic methyl and acetyl marks by postnatal chromium (VI) exposure causes apoptotic changes in the ovary of the F1 offspring. Reprod. Toxicol. 123, 108492. https://doi.org/10.1016/j.reprotox.2023.108492.

Erdem, B., Özkök, A., 2018. Can food supplement produced from apilarnil be an alternative to testosterone replacement therapy? Hacettepe Journal of Biology and Chemistry 45, 635–638. https://doi.org/10.15671/HJBC.2018.207.

Fletcher, E.J., Santacruz-Márquez, R., Mourikes, V.E., Neff, A.M., Laws, M.J., Flaws, J.A., 2022. Effects of phthalate mixtures on ovarian folliculogenesis and steroidogenesis. Toxics 10, 251. https://doi.org/10.3390/toxics10050251.

Fratellone, P.M., Tsimis, F., Fratellone, G., 2016. Apitherapy products for medicinal use. J. Alternative Compl. Med. 22, 1020–1022. https://doi.org/10.1089/acm.2015.0346.

Hajam, Y.A., Rani, R., Ganie, S.Y., Sheikh, T.A., Javaid, D., Qadri, S.S., Pramodh, S., Alsulimani, A., Alkhanani, M.F., Harakeh, S., 2022. Oxidative stress in human pathology and aging: molecular mechanisms and perspectives. Cells 11, 552. https://doi.org/10.3390/cells11030552.

Hama, Y., Ogasawara, Y., Noda, N.N., 2023. Autophagy and cancer: basic mechanisms and inhibitor development. Cancer Sci. 114, 2699–2708. https://doi.org/10.1111/cas.15803.

Hamamci, M., Doganyigit, Z., Silici, S., Okan, A., Kaymak, E., Yilmaz, S., Tokpinar, A., Inan, L.E., 2020. Apilarnil: a novel neuroprotective candidate. Acta Neurol. Taiwanica 29, 33–45.

Hashem, K.S., Elkelawy, A.M.M.H., Abd-Allah, S., Helmy, N.A., 2020. Involvement of Mfn2, Bcl2/Bax signaling and mitochondrial viability in the potential protective effect of royal jelly against mitochondria-mediated ovarian apoptosis by cisplatin in rats. Iranian Journal of Basic Medical Sciences 23, 515. https://doi.org/10.22038/ijbms.2020.40401.9563.

Ibrahim, M.A., Albahlol, I.A., Wani, F.A., Tammam, A.A.-E., Kelleni, M.T., Sayeed, M.U., Abd El-Fadeal, N.M., Mohamed, A.A., 2021. Resveratrol protects against cisplatin-induced ovarian and uterine toxicity in female rats by attenuating oxidative stress, inflammation and apoptosis. Chem. Biol. Interact. 338, 109402. https://doi.org/10.1016/j.cbi.2021.109402.

Jang, H., Lee, O.H., Lee, Y., Yoon, H., Chang, E.M., Park, M., Lee, J.W., Hong, K., Kim, J. O., Kim, N.K., Ko, J.J., Lee, D.R., Yoon, T.K., Lee, W.S., Choi, Y., 2016. Melatonin prevents cisplatin-induced primordial follicle loss via suppression of PTEN/AKT/FOXO3a pathway activation in the mouse ovary. J. Pineal Res. 60, 336–347. https://doi.org/10.1111/jpi.12316.

Jensen, E.C., 2013. Quantitative analysis of histological staining and fluorescence using ImageJ. Anat. Rec. 296, 378–381. https://doi.org/10.1002/ar.22641.

Karakus, S., Ozkaraca, M., 2024. Protective effects of carvedilol against ovarian ischemia-reperfusion injury in rats. Medicine Science 13, 202–208. https://doi.org/10.5455/medscience.2023.10.212.

Karaman, E., Onder, G.O., Goktepe, O., Karakas, E., Mat, O.C., Bolat, D., Koseoglu, E., Tur, K., Baran, M., Ermis, M., 2024. Protective Effects of Boric Acid Taken in Different Ways on Experimental Ovarian İschemia and Reperfusion. Biol. Trace Elem. Res. 202, 2730–2743. https://doi.org/10.1007/s12011-023-03871-1.

Khan, R., Khan, A.Q., Qamar, W., Lateef, A., Tahir, M., Rehman, M.U., Ali, F., Sultana, S., 2012. Chrysin protects against cisplatin-induced colon. toxicity via amelioration of oxidative stress and apoptosis: probable role of p38MAPK and p53. Toxicol. Appl. Pharmacol. 258, 315–329. https://doi.org/10.1016/j.taap.2011.11.013.

Koc, K., Erol, H.S., Colak, S., Cerig, S., Yildirim, S., Geyikoglu, F., 2019. The protective effect of propolis on rat ovary against ischemia-reperfusion injury: immunohistochemical, biochemical and histopathological evaluations. Biomed. Pharmacother. 111, 631–637. https://doi.org/10.1016/j.biopha.2018.12.113.

Kulhan, N., Kulhan, M., Türkler, C., Ata, N., Kiremitli, T., Kiremitli, S., Cimen, F., Süleyman, H., Toprak, V., 2019. Effect of lycopene on oxidative ovary-damage induced by cisplatin in rats. Gen. Physiol. Biophys. 38. https://doi.org/10.4149/gpb_2019006.

Kumariya, S., Ubba, V., Jha, R.K., Gayen, J.R., 2021. Autophagy in ovary and polycystic ovary syndrome: role, dispute and future perspective. Autophagy 17, 2706–2733. https://doi.org/10.1080/15548627.2021.1938914.

Lee, D., Choi, S., Yamabe, N., Kim, K.H., Kang, K.S., 2020. Recent findings on the mechanism of cisplatin-induced renal cytotoxicity and therapeutic potential of natural compounds. Nat. Prod. Sci. 26, 28–49. https://doi.org/10.20307/nps.2020.26.1.28.

Malik, S., Suchal, K., Gamad, N., Dinda, A.K., Arya, D.S., Bhatia, J., 2015. Telmisartan ameliorates cisplatin-induced nephrotoxicity by inhibiting MAPK mediated inflammation and apoptosis. Eur. J. Pharmacol. 748, 54–60. https://doi.org/10.1016/j.ejphar.2014.12.008.

Mentese, A., Alemdar, N.T., Livaoglu, A., Ayazoglu Demir, E., Aliyazicioglu, Y., Demir, S., 2022. Suppression of cisplatin-induced ovarian injury in rats by chrysin: an experimental study. J. Obstet. Gynaecol. 42, 3584–3590. https://doi.org/10.1080/01443615.2022.2130201.

Mete Ural, Ü., Bayoğlu Tekin, Y., Şehitoğlu, İ., Kalkan, Y., Cumhur Cüre, M., 2016. Biochemical, histopathological and immunohistochemical evaluation of the protective and therapeutic effects of thymoquinone against ischemia and ischemia/reperfusion injury in the rat ovary. Gynecol. Obstet. Invest. 81, 47–53. https://doi.org/10.1159/000431220.

Miao, C., Zhao, Y., Chen, Y., Wang, R., Ren, N., Chen, B., Dong, P., Zhang, Q., 2023. Investigation of he's Yang Chao recipe against oxidative stress-related mitophagy and pyroptosis to improve ovarian function. Front. Endocrinol. 14, 1077315. https://doi.org/10.3389/fendo.2023.1077315.

Mundo Rivera, V.M., Tlacuahuac Juárez, J.R., Murillo Melo, N.M., Leyva Garcia, N., Magaña, J.J., Cordero Martínez, J., Jiménez Gutierrez, G.E., 2024. Natural autophagy activators to fight age-related diseases. Cells 13, 1611. https://doi.org/10.3390/cells13191611.

Onder, G.O., Balcioglu, E., Baran, M., Ceyhan, A., Cengiz, O., Suna, P.A., Yıldız, O.G., Yay, A., 2021. The different doses of radiation therapy-induced damage to the ovarian environment in rats. Int. J. Radiat. Biol. 97, 367–375. https://doi.org/10.1080/09553002.2021.1864497.

Özdemir, G., Ersöz, E., Dilek, N., 2021. Apitherapy and health. Black Sea. J. Health Sci. 4, 168–174. https://doi.org/10.19127/bshealthscience.816036.

Perše, M., 2021. Cisplatin mouse models: treatment, toxicity and translatability. Biomedicines 9, 1406. https://doi.org/10.3390/biomedicines9101406.

Pouyanmanesh, F., Nabiuni, M., Nasri, S., Nazari, Z., Karimzadeh, L., 2013. The effect of honey bee venom on levels of lipids and Anti-mullerian hormone in a rat with polycystic ovarian syndrome. Feyz Journal of Kashan University of Medical Sciences 17.

Rafiee, Z., Moaiedi, M.Z., Gorji, A.V., Mansouri, E., 2020. p-Coumaric acid mitigates doxorubicin-induced nephrotoxicity through suppression of oxidative stress, inflammation and apoptosis. Arch. Med. Res. 51, 32–40. https://doi.org/10.1016/j.arcmed.2019.12.004.

Romani, A.M., 2022. Cisplatin in cancer treatment. Biochem. Pharmacol. 206, 115323. https://doi.org/10.1016/j.bcp.2022.115323.

Rutka, I., Galoburda, R., Galins, J., Galins, A., 2021. Bee drone brood homogenate chemical composition and application: a review. Food Sci. (N. Y.) 36, 96–103. https://doi.org/10.22616/rrd.27.2021.014.

Ruslee, S.S., Zaid, S.S.M., Bakrin, I.H., Goh, Y.M., Mustapha, N.M., 2020. Protective effect of Tualang honey against cadmium-induced morphological abnormalities and oxidative stress in the ovary of rats. BMC complementary medicine and therapies 20, 1–11. https://doi.org/10.1186/s12906-020-02960-1.

Safitri, E., Widiyatno, T.V., Prasetyo, R.H., 2016. Honeybee product therapeutic as stem cells homing for ovary failure. Vet. World 9, 1324. https://doi.org/10.14202/vetworld.2016.1324-1330.

Said, R.S., Mantawy, E.M., El-Demerdash, E., 2019. Mechanistic perspective of protective effects of resveratrol against cisplatin-induced ovarian injury in rats: emphasis on anti-inflammatory and anti-apoptotic effects. N. Schmied. Arch. Pharmacol. 392, 1225–1238. https://doi.org/10.1007/s00210-019-01662-x.

Sakin, Ö., Anğın, A.D., Koyuncu, K., Çıkman, M.S., Başak, K., Kaptanağası, A.O., 2020. Protective effects of imatinib and Ginkgo Biloba on cisplatin-induced ovarian damage in rats. Istanbul Medical Journal= Istanbul Tip Dergisi 21, 281. https://doi.org/10.4274/imj.galenos.2020.46667.

Sapmaz, T., Sevgin, K., Topkaraoglu, S., Tekayev, M., Gumuskaya, F., Efendic, F., Pence, M.E., Aktas, S., Hekimoglu, G., Irkorucu, O., 2022. Propolis protects ovarian follicular reserve and maintains the ovary against polycystic ovary syndrome (PCOS) by attenuating degeneration of zona pellucida and fibrous tissue. Biochem. Biophys. Res. Commun. 636, 97–103. https://doi.org/10.1016/j.bbrc.2022.10.098.

Sawczuk, R., Karpinska, J., Miltyk, W., 2019. What do we need to know about drone brood homogenate and what is known. J. Ethnopharmacol. 245, 111581. https://doi.org/10.1016/j.jep.2018.10.04.

Silici, S., 2023. Drone larvae homogenate (Apilarnil) as natural remedy: scientific review. J. Agric. Sci. 29, 947–959. https://doi.org/10.15832/ankutbd.1293015.

Schindelin, J., Arganda-Carreras, I., Frise, E., Kaynig, V., Longair, M., Pietzsch, T., Preibisch, S., Rueden, C., Saalfeld, S., Schmid, B., 2012. Fiji: an open-source platform for biological-image analysis. Nat. Methods 9, 676–682. https://doi.org/10.1038/nmeth.2019.

Spears, N., Lopes, F., Stefansdottir, A., Rossi, V., De Felici, M., Anderson, R., Klinger, F., 2019. Ovarian damage from chemotherapy and current approaches to its protection. Hum. Reprod. Update 25, 673–693. https://doi.org/10.1093/humupd/dmz027.

Topal, E., Strant, M., Yücel, B., Kösoğlu, M., Margaoan, R., Dayıoğlu, M., 2018. Ana ve erkek arı larvalarının biyokimyasal özellikleri ve apiterapötik kullanımı. Hayvansal Üretim 59, 77–82. https://doi.org/10.29185/hayuretim.455478.

Weis, W.A., Ripari, N., Conte, F.L., da Silva Honorio, M., Sartori, A.A., Matucci, R.H., Sforcin, J.M., 2022. An overview about apitherapy and its clinical applications. Phytomedicine 2, 100239. https://doi.org/10.1016/j.phyplu.2022.100239.

Xi, H., Wang, S., Wang, B., Hong, X., Liu, X., Li, M., Shen, R., Dong, Q., 2022. The role of interaction between autophagy and apoptosis in tumorigenesis. Oncol. Rep. 48, 1–16. https://doi.org/10.3892/or.2022.8423.

Xu, B., Guo, W., He, X., Fu, Z., Chen, H., Li, J., Ma, Q., An, S., Li, X., 2024. Repair effect of human umbilical cord mesenchymal stem cell-derived small extracellular vesicles on ovarian injury induced by cisplatin. Environ. Toxicol. https://doi.org/10.1002/tox.24303.

Yalçın, B., Kalkan, K.T., Köseoğlu, E., Karaman, E., Yay, A., 2024. Assessment of the effects of two different doses of methotrexate in rat ovarian tissue: a histological study. Annals of Medical Research 31. https://doi.org/10.5455/annalsmedres.2024.05.098, 582-582.

Zhang, Q.-Y., Wang, F.-X., Jia, K.-K., Kong, L.-D., 2018. Natural product interventions for chemotherapy and radiotherapy-induced side effects. Front. Pharmacol. 9, 1253. https://doi.org/10.3389/fphar.2018.01253.

Zoń, A., Bednarek, I., 2023. Cisplatin in ovarian cancer treatment—known limitations in therapy force new solutions. Int. J. Mol. Sci. 24, 7585. https://doi.org/10.3390/ijms24087585.